PCCP

ROYAL SOCIETY OF CHEMISTRY

PAPER

View Article Online
View Journal

Cite this: DOI: 10.1039/d6cp01222a

Gaunt and Breit two-electron contributions to mean-field transformations and fine structure splitting

Luca Murg, *[ab] Christopher Lane [a] and Roxanne M. Tutchton [a]

Received 2nd April 2026,
Accepted 20th May 2026

DOI: 10.1039/d6cp01222a

rsc.li/pccp

Materials utilized by novel energy systems are often studied using weakly correlated mean-field theories. However, if these systems incorporate heavy elements, relativistic effects must be included. Therefore, a Kramers unrestricted coupled cluster with singles and doubles excitation formalism within a molecular mean-field exact two-component framework (X2C$_{mmf}$) using a four-component Dirac–Hartree–Fock (DHF) reference state is presented. The exact X2C$_{mmf}$ transformed normal-order Hamiltonian incorporates all one-electron and two-electron (2e) contributions from the Coulomb, Gaunt, and Breit operators and is used with the equation of motion method to calculate the excitation energies of the alkali group of elements. Using this framework, the effects of 2e Gaunt and Breit integrals are studied. Results demonstrate growing contributions from these integrals to the generated X2C$_{mmf}$ mean-fields and electronic fine structure calculations with increasing atomic number. Overall, this paper outlines the method, its effect within the X2C$_{mmf}$ approach, and lays the foundation for future theoretical development of relativistic calculations within this framework.

Introduction

Materials relied on by novel energy systems, *e.g.*, generation IV nuclear reactors,[1] are often studied using weakly correlated mean-field theories. In weakly correlated electron systems, the direct Coulomb interaction can be modeled by an effective single-particle potential, *e.g.*, density functional theory. When strong correlations dominate, these mean-field theories can be used as a reference state for various strongly correlated approaches.[2–5] Relativistic effects are typically added perturbatively,[6–8] but this framework is not adequate for systems composed of heavy elements[9–15] and the vast unexplored space of topological materials.[16,17] These deficiencies require us to adjust existing theories to account for a four-component (4c) Dirac reference state[18] utilizing increasingly accurate relativistic Hamiltonians, *e.g.*, the Dirac–Coulomb (DC), Dirac–Coulomb–Gaunt (DCG), and Dirac–Coulomb–Breit (DCB) Hamiltonians. In the no-pair approximation, exact two-component (X2C) transformation theory can be used to decouple the positive energy (pe) and negative energy (ne) spectrum of the Dirac Hamiltonian for wave function-based correlation methods.[19–23] A variety of X2C flavors have been developed most of which fall under the one-electron (1e) X2C framework.[24,25] In the case of the 1eX2C Hamiltonian scheme, the two-electron (2e) interaction terms are omitted from the defining 4c Dirac Hamiltonian resulting in a two-component (2c) Hamiltonian that is "exact" only in the 1e terms. Because the 2e interaction terms are often left untransformed in the 1eX2C basis set, 2e picture-change effects (2ePCEs) will appear.[25] In contrast to the 1eX2C transformation, performed before the self-consistent field (SCF) cycle, molecular mean-field X2C (X2C$_{mmf}$) transformations utilize a unitary decoupling of the 4c molecular mean-field Fock matrix after having converged the 4c SCF DHF equations.[23] Formally, X2C$_{mmf}$ transformation are exact. However, due to the computational cost associated with recomputing and transforming 2e integrals associated with Coulomb (G^{LL}_{LL}, G^{LS}_{LS}, G^{SL}_{SL}, G^{SS}_{SS}) and Gaunt/Breit integrals (G^{SS}_{LL}, G^{SL}_{LS}, G^{LS}_{SL}, G^{LL}_{SS}), previous work using X2C$_{mmf}$ transformations have largely only considered the large component Coulomb integrals in the 2e terms of the X2C$_{mmf}$ transformed normal-order Hamiltonian and often in untransformed form ($G_{+\ +}^{+\ +} \approx G^{LL}_{LL}$). Neglecting or using untransformed 2e interaction terms results in only an approximate X2C$_{mmf}$ transformation.[23,25–27]

This work demonstrates that the Gaunt and Breit 2e integral contribution to the generated mean-field grows as elements become heavier. Furthermore, variations of the X2C$_{mmf}$ transformations including the exact effective 1e DC, DCG, and DCB Fock matrix in-conjunction with the approximate and exact 2e transformed Coulomb, Coulomb–Gaunt, and Coulomb–Breit interaction[23] are computed. Using these X2C$_{mmf}$ transformed

[a] Theoretical Division, Los Alamos National Laboratory, Los Alamos, New Mexico 87545, USA. E-mail: rtutchton@lanl.gov
[b] Department of Nuclear, Plasma, and Radiological Engineering, University of Illinois at Urbana-Champaign, Urbana, USA

normal-order Hamiltonians, we apply Kramers unrestricted coupled cluster (CC) with singles and doubles (SD) excitations.[28–31] The X2C$_{mmf}$-CCSD ground state wave function is then used as a reference for the equation of motion (EOM) method to obtain the excited wave function of the alkali elements.[26,32,33] Results offer insights into the importance of the Gaunt and Breit 2e integral contributions to the 2e terms of the exact X2C$_{mmf}$ transformed normal-order Hamiltonian used in post 4c SCF correlation-excitation steps as elements become heavier.

Theory and methodology

In this work, PySCF's[34,35] implementation of 4c DHF[36,37] using the DC, DCG, and DCB Hamiltonian was used (see Fock matrix in eqn (1)). The 4c DHF calculation enforced the restricted kinetic balance condition[36,37] and used the finite-size nuclear model with a convergence tolerance of 10^{-10} and a max direct inversion of the iterative subspace[38] (DIIS) of 8.

$$\begin{pmatrix} F^{LL} & F^{LS} \\ F^{SL} & F^{SS} \end{pmatrix} \begin{pmatrix} C_L^{+} & C_L^{-} \\ C_S^{+} & C_S^{-} \end{pmatrix} = \begin{pmatrix} I \otimes S & 0 \\ 0 & \frac{1}{2mc^2} I \otimes T \end{pmatrix} \begin{pmatrix} C_L^{+} & C_L^{-} \\ C_S^{+} & C_S^{-} \end{pmatrix} \begin{pmatrix} \varepsilon^{+} & 0 \\ 0 & \varepsilon^{-} \end{pmatrix}, \quad (1)$$

We implemented Kramers unrestricted CCSD (using NumPy)[39,40] employing DIIS following standard CCSD methods for post-SCF wavefunction correlation calculations. The family of relativistic ANO basis sets[41,42] used for this work are obtained from basis set exchange.[43] We note that in 4c DHF, the 2e integral $\hat{g}$ operator takes the following form:

$$\hat{g}_{ij} = \frac{I_4}{r_{ij}} - \frac{1}{2}\left(\frac{\alpha_i \cdot \alpha_j}{r_{ij}} + \frac{\alpha_i \cdot r_{ij} \alpha_j \cdot r_{ij}}{r_{ij}^3}\right). \quad (2)$$

Breit — Coulomb — Gaunt — gauge

The first term in this expression is identified as the typical Coulomb interaction, with the second as Gaunt, and the third as a gauge. The second and third terms are often collectively called the Breit term and are associated with spin–orbit interactions and retardation effects. As dictated by an X2C$_{mmf}$ transformation, after converging the 4c DHF equation, the Hamiltonian for the valence electrons can be written in normal-ordered form,

$$\hat{H}_{X2C_{mmf}} = \sum_{PQ} F_P^Q \left\{a_P^\dagger a_Q\right\} + \frac{1}{4}\sum_{PQRS} V_{PR}^{QS} \left\{a_P^\dagger a_R^\dagger a_S a_Q\right\}, \quad (3)$$

for further use in wave function-based correlation methods.[21,23] The brackets indicate normal ordering with respect to occupied (hole) and virtual (particle) orbitals. The effective 1e terms of the normal-ordered Hamiltonian are elements of the Fock matrix, F_P^Q. The anti-symmetrized electron–electron integrals, $V_{PR}^{QS} = G_{PR}^{QS} - G_{PR}^{SQ}$, represent the 2e contributions to the normal-ordered Hamiltonian. The summation is formally restricted to pe orbitals but in practice, it is further reduced due to truncations of the occupied and virtual space commonly employed in correlated calculations. In this form, it is observed that the matrix elements of the Fock matrix F_P^Q can be obtained from exact decoupling of the corresponding converged 4c molecular Fock matrix. If the basis chosen for the correlation calculation is taken to be the canonical HF orbitals, the list of nonzero matrix elements reduces to the orbital energies $F_P^Q = \varepsilon_P{}^{+}\delta_{PQ}$.[23] Similarly, we restricted ourselves to the pe 2e interaction terms, $G_{++}{}^{++}$. These can be obtained for the Coulomb integrals as $G_{++}{}^{++} = C_L^{\dagger,+}C_L^{\dagger,+}G_{LL}^{LL}C_L{}^{+}C_L{}^{+} + C_L^{\dagger,+}C_S^{\dagger,+}G_{LS}^{LS}C_L{}^{+}C_S{}^{+} + C_S^{\dagger,+}C_L^{\dagger,+}G_{SL}^{SL}C_S{}^{+}C_L{}^{+} + C_S^{\dagger,+}C_S^{\dagger,+}G_{SS}^{SS}C_S{}^{+}C_S{}^{+}$ and for Gaunt/Breit as $G_{++}{}^{++} = C_L^{\dagger,+}C_L^{\dagger,+}G_{LL}^{SS}C_S{}^{+}C_S{}^{+} + C_L^{\dagger,+}C_S^{\dagger,+}G_{LS}^{SL}C_S{}^{+}C_L{}^{+} + C_S^{\dagger,+}C_L^{\dagger,+}G_{SL}^{LS}C_L{}^{+}C_S{}^{+} + C_S^{\dagger,+}C_S^{\dagger,+}G_{SS}^{LL}C_L{}^{+}C_L{}^{+}$.[23] All X2C$_{mmf}$ transformed normal-order Hamiltonians used in this study are exact in the 1e Fock term (labeled-1e). X2C$_{mmf}$ transformed normal-order Hamiltonians that are also exact in the 2e interaction terms are labeled-1e2e and account for all Coulomb integrals (G_{LL}^{LL}, G_{LS}^{LS}, G_{SL}^{SL}, G_{SS}^{SS}) and Gaunt/Breit integrals (if used at 4c SCF level, G_{LL}^{SS}, G_{LS}^{SL}, G_{SL}^{LS}, G_{SS}^{LL}). Nonexact 2e interaction terms in the X2C$_{mmf}$ transformed normal-ordered Hamiltonians account only for the transformed Coulomb integrals (G_{LL}^{LL}, G_{LS}^{LS}, G_{SL}^{SL}, G_{SS}^{SS}). These variations of X2C$_{mmf}$ transformed normal-order Hamiltonians are defined in Table 1.

After X2C$_{mmf}$, Kramers unrestricted CC theory is used to approximate the true wave function by systematically mixing in excited configurations. The wave function in CC theory is defined as $|\Psi\rangle = e^{\hat{T}}|\Phi_{X2C_{mmf},0}\rangle$ where $|\Phi_{X2C_{mmf},0}\rangle$ is the single determinant wave function.[21,44] For this work, the cluster operator $\hat{T}$ was truncated to the SD hole-particle excitations $\hat{T} = \hat{T}_1 + \hat{T}_2$ where $\hat{T}_1 = \sum_i \sum_a t_a^i \hat{a}_a^\dagger \hat{a}_i$ and $\hat{T}_2 = \frac{1}{4}\sum_{ij}\sum_{ab} t_{ab}^{ij} \hat{a}_a^\dagger \hat{a}_b^\dagger \hat{a}_j \hat{a}_i$. Using the similarity transformed Hamiltonian, $\tilde{H} = e^{-\hat{T}}\hat{H}_{X2C_{mmf}}e^{\hat{T}}$, one can solve for the SD excitation amplitudes, t_a^i and t_{ab}^{ij} through various subspace projections listed in eqn (4)–(6),[21,39,40,45–48]

$$\langle \Phi_{X2C_{mmf},0}|\tilde{H}|\Phi_{X2C_{mmf},0}\rangle = E, \quad (4)$$

$$\langle \Phi_{X2C_{mmf},0}|\hat{a}_i^\dagger \hat{a}_a \tilde{H}|\Phi_{X2C_{mmf},0}\rangle = 0, \quad (5)$$

$$\langle \Phi_{X2C_{mmf},0}|\hat{a}_i^\dagger \hat{a}_j^\dagger \hat{a}_b \hat{a}_a \tilde{H}|\Phi_{X2C_{mmf},0}\rangle = 0. \quad (6)$$

It is important to note that the asymmetric CCSD equations do not satisfy the variational principle due to the truncation of the cluster operators. This means that the calculated energy will not necessarily be an upper bound for the exact energy.[49] The Kramers unrestricted CCSD implementation was benchmarked

Table 1 X2C$_{mmf}$ transformation used in study as well as their contributions to 1-electron and 2-electron terms

X2C$_{mmf}$ type	1-Electron	2-Electron contribution
DC-1e2e	Coulomb	Coulomb
DCG-1e	Coulomb–Gaunt	Coulomb
DCB-1e	Coulomb–Breit	Coulomb
DCG-1e2e	Coulomb–Gaunt	Coulomb–Gaunt
DCB-1e2e	Coulomb–Breit	Coulomb–Breit

Table 2 Electronic fine structure splitting $\left({}^2P_{\frac{3}{2}} - {}^2P_{\frac{1}{2}}\right)$ for varying atom types, basis types, and X2C$_{mmf}$ transformation types, calculated using EOM-CCSD-X2C$_{mmf}$-DHF and compared to experiment (units are eV)

Atom	Basis	Experiment	DC-1e2e	DCG-1e	DCB-1e	DCG-1e2e	DCB-1e2e
Na	ANO-RCC-MB	0.0021	0.0030	0.0028	0.0028	0.0028	0.0028
Na	ANO-RCC-VDZ	0.0021	0.0023	0.0022	0.0022	0.0022	0.0022
Na	ANO-RCC-VDZP	0.0021	0.0024	0.0022	0.0022	0.0022	0.0022
Na	ANO-RCC-VTZP	0.0021	0.0023	0.0022	0.0022	0.0022	0.0022
Na	ANO-RCC-VQZP	0.0021	0.0023	0.0022	0.0022	0.0022	0.0022
K	ANO-RCC-MB	0.0072	0.0074	0.0072	0.0072	0.0072	0.0072
K	ANO-RCC-VDZ	0.0072	0.0066	0.0064	0.0064	0.0064	0.0064
K	ANO-RCC-VDZP	0.0072	0.0077	0.0075	0.0075	0.0075	0.0075
K	ANO-RCC-VTZP	0.0072	0.0076	0.0074	0.0074	0.0074	0.0074
Rb	ANO-RCC-MB	0.0295	0.0220	0.0220	0.0219	0.0220	0.0219
Rb	ANO-RCC-VDZ	0.0295	0.0235	0.0232	0.0232	0.0232	0.0232
Rb	ANO-RCC-VDZP	0.0295	0.0240	0.0237	0.0237	0.0237	0.0237
Cs	ANO-RCC-MB	0.0687	0.0508	0.0513	0.0512	0.0513	0.0512
Cs	ANO-RCC-VDZ	0.0687	0.0529	0.0529	0.0529	0.0529	0.0529
Fr	ANO-RCC-VDZ	0.2091	0.1543	0.1566	0.1563	0.1566	0.1563

using PySCF implementation of CCSD. Both the developed CCSD code and PySCF's implementation used the same X2C$_{mmf}$ transformed normal-ordered Hamiltonian as the single determinant reference state. The results of these calculations can be seen in Tables S7–S10 in the supplementary information, which used a convergence tolerance of 10^{-11} and max DIIS of 8). From these tables it is observed that all converged values match to convergence tolerance. Using the CCSD ground-state wave function and noting that $\tilde{H}$ is not Hermitian, one can define the excited wave function using

$$\hat{R}_I|\Psi\rangle = e^{\hat{T}}\left(r_0 + \sum_i\sum_a r_i^a \hat{a}_a^\dagger \hat{a}_i + \frac{1}{4}\sum_{ij}\sum_{ab} r_{ij}^{ab}\hat{a}_a^\dagger \hat{a}_b^\dagger \hat{a}_j \hat{a}_i\right)|\Phi_{X2C_{mmf},0}\rangle, \quad (7)$$

$$\langle\tilde{\Psi}|\hat{L}_I = \langle\Phi_{X2C_{mmf},0}|\left(l_0 + \sum_i\sum_a l_a^i \hat{a}_a^\dagger \hat{a}_i + \frac{1}{4}\sum_{ij}\sum_{ab} l_{ab}^{ij}\hat{a}_a^\dagger \hat{a}_b^\dagger \hat{a}_j \hat{a}_i\right)e^{-\hat{T}}, \quad (8)$$

where I represents the Ith excited state.[27,32,33] Similar to CCSD, this procedure truncates the operators and assumes that the CCSD ground state captures the dominant dynamical correlations such that the excited states can be represented as excitations on top of the correlated vacuum. These bra and ket states, although not orthonormal among themselves, satisfy biorthogonality $\langle\Phi_{X2C_{mmf},0}|\hat{L}_I e^{-\hat{T}}e^{\hat{T}}\hat{R}_J|\Phi_{X2C_{mmf},0}\rangle = C\delta_{IJ}$ and by choosing C to be unity to one can enforce normalization. Defining the normal-ordered similarity transformed Hamiltonian as $\bar{H} = \tilde{H} - E$ one can solve for the expansion coefficients r_0, r_i^a, r_{ij}^{ab}, l_0, l_a^i, and l_{ab}^{ij} using eqn (9) and (10),

$$\bar{H}\hat{R}_I|\Phi_{X2C_{mmf},0}\rangle = \omega_I\hat{R}_I|\Phi_{X2C_{mmf},0}\rangle, \quad (9)$$

$$\langle\Phi_{X2C_{mmf},0}|\hat{L}_I\bar{H} = \langle\Phi_{X2C_{mmf},0}|\hat{L}_I\omega_I, \quad (10)$$

where ω_I is the difference in energy between the Ith excited state and E. In this study, PySCF[34,35] implementation of EOM was used and we refer the reader to their open source code for details of their implementation. Using EOM-CCSD-X2C$_{mmf}$-DHF, we calculated the ${}^2S_{\frac{1}{2}} \rightarrow {}^2P_{\frac{1}{2}}$ excitations for the alkali elements. Results of these calculations are consistent with experimental values, see in Table S1 and Table 2, and a similar study[32] using the Kramers unrestricted EOM-CCSD-X2C$_{mmf}$-DHF, a point-nucleus charge, and the X2C$_{mmf}$ untransformed DC-1e, and DCB-1e Hamiltonian for Na, K, and Rb in the ANO basis sets.

Analysis of results

The influence of the Gaunt and Breit 2e integrals on their respective DHF–DCG and DHF–DCB mean-fields is quantified using the mean squared displacement of the pe eigenvalue spectrum (ε^+) of the 4c Fock (labeled $\varepsilon_{DHF}{}^+$) and decoupled 2c Fock matrix. The $\varepsilon_{DCG\text{-}1e}{}^+$, $\varepsilon_{DCB\text{-}1e}{}^+$ represent decoupled 2c pe Fock spectrum which are exact in all one-body terms but neglect two-body Gaunt and Breit integrals respectively in

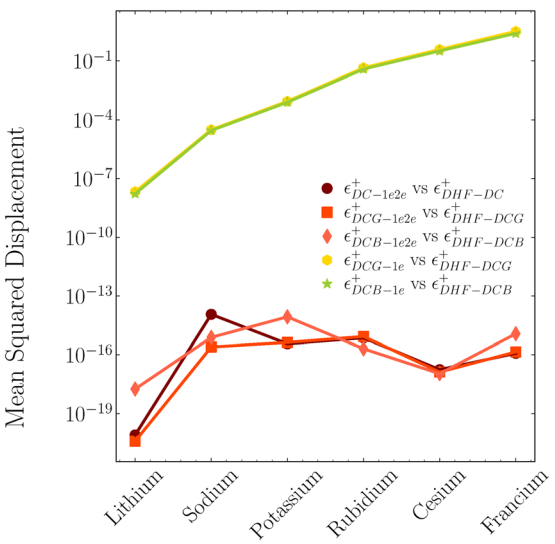

Fig. 1 Mean squared displacement of positive energy spectrum after X2C$_{mmf}$ using DC-1e2e, DCG-1e, and DGB-1e, DCG-1e2e, and DCB-1e2e transformation *versus* the respective positive energy spectrum from 4c DHF using DC, DCG, and DCB Hamiltonian in ANO-RCC-VDZ basis set (MSD $= \frac{1}{n}\sum_{i=1}^{n}\left|\varepsilon_{i,4c\text{-}DHF}{}^+ - \varepsilon_{i,2c}{}^+\right|^2$, units are Hartree).

decoupling while $\varepsilon_{\text{DC-1e2e}}^{+}$, $\varepsilon_{\text{DCG-1e2e}}^{+}$, $\varepsilon_{\text{DCB-1e2e}}^{+}$ represent the exactly decoupled 2c pe Fock spectrum. Results of these calculations are seen in Fig. 1 (Fig. S1 in the supplementary information demonstrates results are independent of basis choice). Here, we find $\varepsilon_{\text{DCG-1e}}^{+,2c}$ *vs.* $\varepsilon_{\text{DHF-DCG}}^{+}$ and $\varepsilon_{\text{DCB-1e}}^{+}$ *vs.* $\varepsilon_{\text{DHF-DCB}}^{+}$ to exhibit a growing discrepancy in the pe eigenvalue spectrum while the exactly decoupled 2c have consistent negligible error. This confirms that Gaunt and Breit integrals increasingly contribute to their respective 4c DHF mean-field as elements become heavier.

A similar procedure can be performed to quantify discrepancies in 4c DHF mean fields using higher order relativistic corrections (DC, DCG, and DCB) with increasing atomic number. This is accomplished using the mean squared displacement of the pe eigenvalue spectrum (ε^{+}) of the 4c DHF–DCB Fock (labeled $\varepsilon_{\text{DHF-DCB}}^{+}$) and various decoupled 2c Fock introduced above ($\varepsilon_{\text{DCG-1e}}^{+}$, $\varepsilon_{\text{DCB-1e}}^{+}$, $\varepsilon_{\text{DC-1e2e}}^{+}$, $\varepsilon_{\text{DCG-1e2e}}^{+}$, $\varepsilon_{\text{DCB-1e2e}}^{+}$). Fig. 2 shows the results of mean squared displacement analysis while Fig. S2 (see supplementary information) shows results are independent of basis choice. Observing a growing displacement in pe eigenvalue spectrum neglecting Gaunt or gauge ($\varepsilon_{\text{DHF-DCB}}^{+}$ *vs.* $\varepsilon_{\text{DCG-1e}}^{+}$, $\varepsilon_{\text{DCB-1e}}^{+}$, $\varepsilon_{\text{DC-1e2e}}^{+}$, $\varepsilon_{\text{DCG-1e2e}}^{+}$), a lower displacement in spectrum exact in Gaunt ($\varepsilon_{\text{DHF-DCB}}^{+}$ *vs.* $\varepsilon_{\text{DCG-1e2e}}^{+}$), and a negligible displacement in the exactly decoupled spectrum including both Gaunt and gauge ($\varepsilon_{\text{DHF-DCB}}^{+}$ *vs.* $\varepsilon_{\text{DCB-1e2e}}^{+}$), confirms an increasing discrepancy in pe mean field obtained using 4c DHF–DC, DHF–DCG, or DHF–DCB with increasing atomic number. This result emphasizes the need for increasingly accurate Hamiltonian as atomic number increases.

Moving on to the EOM-CCSD-X2C$_{\text{mmf}}$-DHF calculations, it is of interest to understand the impact of the Gaunt and Breit integrals on the 1e and 2e terms of X2C$_{\text{mmf}}$ transformed normal-ordered Hamiltonians used in post 4c SCF correlation-excitations steps.

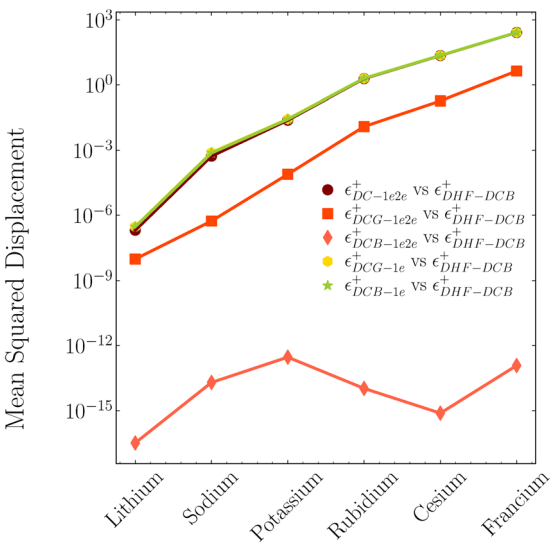

Fig. 2 Mean squared displacement of positive energy spectrum after X2C$_{\text{mmf}}$ using DC-1e2e, DCG-1e, and DGB-1e, DCG-1e2e, and DCB-1e2e transformation *versus* the absolute value of positive energy spectrum from 4c DHF using the DCB Hamiltonian in ANO-RCC-VDZ basis set ($\text{MSD} = \frac{1}{n}\sum_{i=1}^{n}\left|\varepsilon_{i,\text{4c-DHF-DCB}}^{+} - \varepsilon_{i,\text{2c}}^{+}\right|^{2}$, units are Hartree).

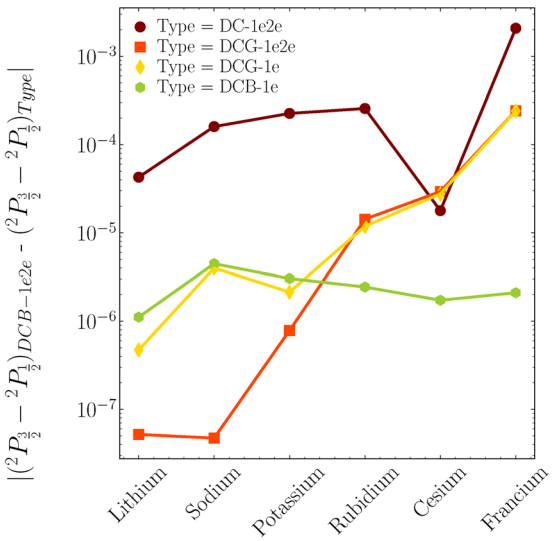

Fig. 3 Absolute difference of fine structure splitting predicted using the DC-1e2e, DCG-1e, DCB-1e, and DCG-1e2e transformation *versus* the DCB-1e2e transformation for various basis sets calculated using EOM-CCSD-X2C$_{\text{mmf}}$-DHF in ANO-RCC-VDZ basis set (units are eV).

Table 2 shows electronic fine structure (EFS, ${}^{2}P_{\frac{3}{2}} - {}^{2}P_{\frac{1}{2}}$) for varying atom types, basis types, and X2C$_{\text{mmf}}$ transformation types, calculated using EOM-CCSD-X2C$_{\text{mmf}}$-DHF and compared to experiment. Table 2 demonstrates that error of the predicted and experimental EFS decreases with increasingly accurate basis sets (ANO-RCC-VDZ → ANO-RCC-VDZP → ANO-RCC-VTZP → ANO-RCC-VQZP). Table 2 further demonstrates that as elements increase in atomic number, predictions deviate from experiment. These deviations can likely be attributed the neglect of important higher-order excitations necessary for modeling heavier elements.[50] However, for small elements (Na,K), where a CCSD framework is sufficient to provide a reasonable reconstruction of correlation, it is noted that more accurate X2C$_{\text{mmf}}$ transformed normal-ordered Hamiltonians provide a better prediction of the EFS.

Fig. 3 presents results of the absolute difference between the EFS $\left({}^{2}P_{\frac{3}{2}} - {}^{2}P_{\frac{1}{2}}\right)$ predicted by DC-1e2e, DCG-1e, DCB-1e, and DCG-1e2e *versus* the EFS predicted by DCB-1e2e transformation (supplementary Fig. S3 demonstrates results are independent of basis choice). Fig. 3 and Table 2 both indicate that even for elements with small atomic number, including only the Coulomb integrals is insufficient, the Gaunt integrals in both the 1e and 2e terms of the X2C$_{\text{mmf}}$ transformed normal ordered Hamiltonian contribute in 3rd–4th decimal of EFS prediction within the EOM-CCSD-X2C$_{\text{mmf}}$-DHF framework. Additionally, as elements increase in atomic number, the contributions of the gauge integrals in the 1e and 2e term of the X2C$_{\text{mmf}}$ transformed normal ordered Hamiltonian contribute in 4th–5th decimal of EFS prediction.

Closing remarks

As higher fidelity electronic structure is needed, the introduction of relativistic theories becomes increasingly important to

characterize certain systems. In order to address this issue, we developed a CCSD code using the 4c DHF ground state and $X2C_{mmf}$ transformed normal-order Hamiltonian incorporating all 1e and 2e contributions from the Coulomb, Gaunt, and Breit operators. Results confirm that Gaunt and Breit integrals increasingly contribute to the DHF solutions causing deviations with increasing atomic number in the mean fields generated with varying orders of relativistic corrections (DC, DCG, and DCB). It is also shown that for elements with small atomic number, the Gaunt integrals in both the 1e and 2e terms of the $X2C_{mmf}$ transformed normal ordered Hamiltonian contribute significantly to EFS predictions within the EOM-CCSD-$X2C_{mmf}$-DHF framework while those elements with increasing atomic number have non-negligible contributions of the gauge integrals. Overall, this work outlines limitations of various $X2C_{mmf}$ transformations, and lays the ground work for more studies utilizing the DCB Hamiltonian within an exact X2C mean-field approach.

Conflicts of interest

There are no conflicts to declare.

Data availability

The data supporting the conclusions of this article are contained within the manuscript and its supplementary information (SI). Supplementary information is available. See DOI: https://doi.org/10.1039/d6cp01222a. This contains additional calculation results and extended analysis.

Acknowledgements

This work was carried out under the auspices of the U.S. Department of Energy (DOE) National Nuclear Security Administration (NNSA) under Contract No. 89233218CNA000001. It was supported by the G.T Seaborg Institute for Transactium Science at Los Alamos National Laboratory (L.M.), the LANL LDRD program (C. L. and R. M. T), and in part by the Center for Integrated Nanotechnologies, a DOE BES user facility, in partnership with the LANL Institutional Computing Program for computational resources.

References

1 L. Murg, S. C. Lee and V. F. Grizzi, *et al.*, Enhanced exploration of LiF–NaF thermal conductivity through transferable equivariant graph neural networks, *J. Appl. Phys.*, 2025, **137**, 064701.
2 B. Himmetoglu, A. Floris, S. De Gironcoli and M. Cococcioni, Hubbard-corrected DFT energy functionals: The LDA+U description of correlated systems, *Int. J. Quantum Chem.*, 2014, **114**, 14–49.
3 A. Georges, G. Kotliar, W. Krauth and M. J. Rozenberg, Dynamical mean-field theory of strongly correlated fermion systems and the limit of infinite dimensions, *Rev. Mod. Phys.*, 1996, **68**, 13.
4 A. Wodynski and M. Kaupp, Local hybrid functional applicable to weakly and strongly correlated systems, *J. Chem. Theory Comput.*, 2022, **18**, 6111–6123.
5 P. Rivero, I. D. P. Moreira, G. E. Scuseria and F. Illas, Description of magnetic interactions in strongly correlated solids via range-separated hybrid functionals, *Phys. Rev. B:Condens. Matter Mater. Phys.*, 2009, **79**, 245129.
6 B. A. Heß, C. M. Marian, U. Wahlgren and O. Gropen, A mean-field spin-orbit method applicable to correlated wavefunctions, *Chem. Phys. Lett.*, 1996, **251**, 365–371.
7 P. Schwerdtfeger, *Relativistic Electronic Structure Theory, Part 1: Fundamentals*, Elsevier Science, 2002, pp. 1–926.
8 K. Klein and J. Gauss, Perturbative calculation of spin-orbit splittings using the equation-of-motion ionization-potential coupled-cluster ansatz, *J. Chem. Phys.*, 2008, **129**, 194106.
9 R. M. Tutchton, W.-T. Chiu, R. C. Albers, G. Kotliar and J.-X. Zhu, Electronic correlation induced expansion of Fermi pockets in δ-plutonium, *Phys. Rev. B*, 2020, **101**, 245156.
10 P. Pyykko, Relativistic effects in structural chemistry, *Chem. Rev.*, 1988, **88**, 563–594.
11 T. Saue, Relativistic Hamiltonians for chemistry: A primer, *ChemPhysChem*, 2011, **12**, 3077–3094.
12 J. Autschbach, Perspective: relativistic effects, *J. Chem. Phys.*, 2012, **136**, 150902.
13 P. Pyykkö, Relativistic effects in chemistry: more common than you thought, *Annu. Rev. Phys. Chem.*, 2012, **63**, 45–64.
14 W. Liu, Advances in relativistic molecular quantum mechanics, *Phys. Rep.*, 2014, **537**, 59–89.
15 D. Jayatilaka and T. J. Lee, The form of spin orbitals for open-shell restricted Hartree–Fock reference functions, *Chem. Phys. Lett.*, 1992, **199**, 211–219.
16 T. Fukui and Y. Hatsugai, Topological aspects of the quantum spin-Hall effect in graphene: Z 2 topological order and spin Chern number, *Phys. Rev. B:Condens. Matter Mater. Phys.*, 2007, **75**, 121403.
17 J. G. Rau, E. K. H. Lee and H. Y. Kee, Spin-orbit physics giving rise to novel phases in correlated systems: Iridates and related materials, *Annu. Rev. Condens. Matter Phys.*, 2016, **7**, 195–221.
18 B. Swirles, The relativistic self-consistent field, *Proc. R. Soc. London, Ser. A*, 1935, **152**, 625–649.
19 J. Liu, Y. Shen, A. Asthana and L. Cheng, Two-component relativistic coupled-cluster methods using mean-field spin-orbit integrals, *J. Chem. Phys.*, 2018, **148**, 034106.
20 A. Asthana, J. Liu and L. Cheng, Exact two-component equation-of-motion coupled-cluster singles and doubles method using atomic mean-field spin-orbit integrals, *J. Chem. Phys.*, 2019, **150**, 074102.
21 J. V. Pototschnig, A. Papadopoulos, D. I. Lyakh, M. Repisky, L. Halbert, A. Severo Pereira Gomes, H. J. A. Jensen and L. Visscher, Implementation of relativistic coupled cluster theory for massively parallel GPU-accelerated computing architectures, *J. Chem. Theory Comput.*, 2021, **17**, 5509–5529.
22 P. Tecmer, A. Severo Pereira Gomes, S. Knecht and L. Visscher, Communication: Relativistic Fock-space

coupled cluster study of small building blocks of larger uranium complexes, *J. Chem. Phys.*, 2014, **141**, 041107.
23 J. Sikkema, L. Visscher, T. Saue and M. Iliaš, The molecular mean-field approach for correlated relativistic calculations, *J. Chem. Phys.*, 2009, **131**, 124116.
24 D. Peng and M. Reiher, Exact decoupling of the relativistic Fock operator, *Theor. Chem. Acc.*, 2012, **131**, 1081.
25 S. Knecht, M. Repisky, H. J. A. Jensen and T. Saue, Exact two-component Hamiltonians for relativistic quantum chemistry: Two-electron picture-change corrections made simple, *J. Chem. Phys.*, 2022, **157**, 114106.
26 T. Saue, R. Bast, A. S. P. Gomes, H. J. A. Jensen, L. Visscher, I. A. Aucar, R. Di Remigio, K. G. Dyall, E. Eliav and E. Fasshauer, *et al.*, The DIRAC code for relativistic molecular calculations, *J. Chem. Phys.*, 2020, **152**, 204104.
27 T. Zhang, S. Banerjee, L. N. Koulias, E. F. Valeev, A. E. DePrince III and X. Li, Dirac-Coulomb-Breit Molecular Mean-Field Exact-Two-Component Relativistic Equation-of-Motion Coupled-Cluster Theory, *J. Phys. Chem. A*, 2024, **128**, 3408–3418.
28 J. Čížek, On the correlation problem in atomic and molecular systems. Calculation of wavefunction components in Ursell-type expansion using quantum-field theoretical methods, *J. Chem. Phys.*, 1966, **45**, 4256–4266.
29 J. Čížek, On the use of the cluster expansion and the technique of diagrams in calculations of correlation effects in atoms and molecules, *Adv. Chem. Phys.*, 1969, **14**, 35–89.
30 J. Čížek and J. Paldus, Correlation problems in atomic and molecular systems III. Rederivation of the coupled-pair many-electron theory using the traditional quantum chemical methodst, *Int. J. Quantum Chem.*, 1971, **5**, 359–379.
31 R. J. Bartlett and M. Musiał, Coupled-cluster theory in quantum chemistry, *Rev. Mod. Phys.*, 2007, **79**, 291–352.
32 S. H. Yuwono, R. R. Li, T. Zhang, X. Li and A. E. DePrince, Two-component relativistic equation-of-motion coupled cluster for electron ionization, *J. Chem. Phys.*, 2025, **162**, 084110.
33 J. F. Stanton and R. J. Bartlett, The equation of motion coupled-cluster method. A systematic biorthogonal approach to molecular excitation energies, transition probabilities, and excited state properties, *J. Chem. Phys.*, 1993, **98**, 7029–7039.
34 Q. Sun, T. C. Berkelbach, N. S. Blunt, G. H. Booth, S. Guo, Z. Li, J. Liu, J. D. McClain, E. R. Sayfutyarova and S. Sharma, *et al.*, PySCF: the Python-based simulations of chemistry framework, *Wiley Interdiscip. Rev.: Comput. Mol. Sci.*, 2018, **8**, e1340.
35 Q. Sun, X. Zhang, S. Banerjee, P. Bao, M. Barbry, N. S. Blunt, N. A. Bogdanov, G. H. Booth, J. Chen and Z.-H. Cui, *et al.*, Recent developments in the PySCF program package, *J. Chem. Phys.*, 2020, **153**, 024109.
36 S. Sun, T. F. Stetina, T. Zhang, H. Hu, E. F. Valeev, Q. Sun and X. Li, Efficient Four-Component Dirac-Coulomb-Gaunt Hartree-Fock in the Pauli Spinor Representation, *J. Chem. Theory Comput.*, 2021, **17**, 3388–3402.
37 S. Sun, J. Ehrman, Q. Sun and X. Li, Efficient evaluation of the Breit operator in the Pauli spinor basis, *J. Chem. Phys.*, 2022, **157**, 064112.
38 P. Császár and P. Pulay, Geometry optimization by direct inversion in the iterative subspace, *J. Mol. Struct.*, 1984, **114**, 31–34.
39 L. Visscher, K. G. Dyall and T. J. Lee, Kramers-restricted closed-shell CCSD theory, *Int. J. Quantum Chem.*, 1995, **56**, 411–419.
40 L. Visscher, T. J. Lee and K. G. Dyall, Formulation and implementation of a relativistic unrestricted coupled-cluster method including noniterative connected triples, *J. Chem. Phys.*, 1996, **105**, 8769–8776.
41 B. O. Roos, R. Lindh, P. Å. Malmqvist, V. Veryazov and P. O. Widmark, Main group atoms and dimers studied with a new relativistic ANO basis set, *J. Phys. Chem. A*, 2004, **108**, 2851–2858.
42 B. O. Roos, R. Lindh, P. Å. Malmqvist, V. Veryazov and P. O. Widmark, New relativistic ANO basis sets for transition metal atoms, *J. Phys. Chem. A*, 2005, **109**, 6575–6579.
43 B. P. Pritchard, D. Altarawy, B. Didier, T. D. Gibson and T. L. Windus, New basis set exchange: An open, up-to-date resource for the molecular sciences community, *J. Chem. Inf. Model.*, 2019, **59**, 4814–4820.
44 I. Shavitt and R. J. Bartlett, *Many-body methods in chemistry and physics: MBPT and coupled-cluster theory*, Cambridge University Press, 2009.
45 R. J. Bartlett, Coupled-cluster theory and its equation-of-motion extensions, *Wiley Interdiscip. Rev.: Comput. Mol. Sci.*, 2012, **2**, 126–138.
46 J. Cizek, On the Correlation Problems in Atomic and Molecular Systems. Calculation of Wavefunction Components in Ursell-Type Expansion Using Quantum-Field Theoretical Methods, *J. Chem. Phys.*, 1966, **45**(11), 4256–4266.
47 G. D. Purvis and R. J. Bartlett, A full coupled-cluster singles and doubles model: The inclusion of disconnected triples, *J. Chem. Phys.*, 1982, **76**, 1910–1918.
48 R. J. Bartlett, Coupled-cluster approach to molecular structure and spectra: a step toward predictive quantum chemistry, *J. Phys. Chem.*, 1989, **93**, 1697–1708.
49 T. D. Crawford and H. F. Schaefer III, An introduction to coupled cluster theory for computational chemists, *Rev. Comput. Chem.*, 2007, **14**, 33–136.
50 I. Magoulas, J. Shen and P. Piecuch, Addressing strong correlation by approximate coupled-pair methods with active-space and full treatments of three-body clusters, *Mol. Phys.*, 2022, **120**, e2057365.

